

Modeling Slope Stability in Honduras: Parameter Sensitivity and Scale of Aggregation

Benjamin F. Zaitchik, Harold M. van Es,* and Patrick J. Sullivan

ABSTRACT

Hurricane Mitch (1998) was the deadliest storm to strike the western hemisphere in over 200 yr, and landslides were a significant component of the storm impact, inflicting direct damage on steep lands and triggering mudslides that devastated valleys below. The stability index mapping (SINMAP) model was applied to a 46.1-km² agricultural area in Central Honduras to predict the spatial distribution of shallow debris slides based on the infinite slope stability model and a steady-state hydrology module. The region was surveyed for geology and depth of bedrock, and 63 soil samples were collected on which bulk density, saturated shear strength, angle of soil friction, and saturated hydraulic conductivity were measured. A digital elevation model (DEM) was developed from digitized elevation contours. The natural variability of soil properties was accounted for in a set of model simulations based on parameter distributions, and results were presented in a distributed probability map (DPM) for slope failure that, in turn, was used to identify the spatial scale of variability captured by the model. Ripley's *K*-function for distribution of a spatial point process was applied to mapped landslides and to simulated data based on the DPM. Observed landslide locations were more tightly clustered than those predicted by the physically based model, indicating that fine-scale physical phenomena not captured by the model likely play a role in slope failure. Aggregation of observed landslides on a scale of 150 m made the comparison with model predictions more consistent. Both parameter variability and inventory scale are important considerations in the evaluation of a slope stability model.

LANDSLIDES are a source of severe natural disturbance and societal hazard in humid regions throughout the world (Guariguata, 1990; Bergin et al., 1995; Walker et al., 1996; Iida, 1999). In addition to degrading agricultural lands (Lal, 1994), disrupting transportation (Lloyd et al., 1994), and causing immediate damage to infrastructure (Royster, 1979), landslide activity can be the dominant denudational process on humid hillslopes (Iida, 1999; Pla, 1997; Simon et al., 1990), contributing significantly to the sedimentation of reservoirs (Nagle et al., 1999). This sedimentation represents a serious economic threat, as the cost of remedying sedimentation in the reservoirs of the world's hydroelectric dams—estimated at \$130 billion over a decade ago (Mahmood, 1987)—far exceeds direct economic loss because of landslide activity, estimated at \$2 to 5 billion annually (Schuster, 1994). Landslides also extract a significant human toll in poorer nations. Over 95% of all fatalities related to landslides occur in developing countries (Hansen, 1994), and population growth has forced increasing occupation of landslide-prone slopes, especially by the urban and rural poor (Pellek, 1989).

Hurricane Mitch (October 1998) was the strongest hurricane to strike the Atlantic basin in 10 yr, but it also came to be the most deadly storm in the western hemisphere in over 200 yr. There were more than 11 000 storm-related deaths in Central America and the Caribbean (McCown et al., 1998), and the lasting impact on health and security in the region is inestimable (Inter-American Development Bank [IADB], 1999). Local and international aid agencies have stressed risk mitigation as an essential component of any recovery effort, including improved watershed management, vulnerability assessment, and environmental awareness on the community and institutional level (IADB, 1999). Appropriate application of geographical information systems (GIS) and environmental models can play a key role in such risk mitigation initiatives (Coppock, 1995), but to date management-oriented hazard models have been applied in the developing world only rarely and with mixed success (Alexander, 1995; Chung et al., 1995), “in large part because” of limitations in relevant historical and biophysical data (Coppock, 1995).

Landslide Model Uncertainty and Scale

Geographical information systems can be highly useful in landslide modeling, as the endeavor requires spatially complete information on topography, soil strength, and hydrology for the entire area of interest, but GIS-based approaches are plagued by a susceptibility to error magnification stemming from broad estimation of parameters (Grayson et al., 1992), deaggregation of spatially averaged data (Miles et al., 2000), and error propagation in distributed models (Coppock, 1995). Sensitivity and error analyses are therefore essential to ensure the reliability of management-directed models (Coppock, 1995; Heuvelink and Burrough, 1992). The caveat is particularly significant for landslide susceptibility models, because research modelers commonly report model predictions in binary or deterministic terms even when variability has been recognized in sensitivity analyses (Miles et al., 2000; Gorsevski et al., 2000; Wu and Sidle, 1995; Montgomery and Dietrich, 1994). To avoid any pretense of certainty, application-oriented modelers often prefer qualitative stability classes to numeric indices (Dunne, 1998). This approach appropriately engages the end-user in management decisions, but stability classes can be highly generalized or difficult to interpret (e.g., Roy, 2001; Wang and Unwin, 1992; Jibson et al., 1993).

A quantitative representation of model uncertainty would be preferable. For statistical models this can be

Benjamin F. Zaitchik and Harold M. van Es, Department of Crop and Soil Science, and Patrick J. Sullivan, Department of Natural Resources, Cornell University, Ithaca, NY 14850. Received 30 July 2001. *Corresponding author (hmv1@cornell.edu).

Abbreviations: DEM, digital elevation model; DPM, distributed probability map; GIS, geographical information system; IADB, Inter-American Development Bank; SD, standard deviation; SINMAP, stability index mapping.

achieved through probabilistic prediction methods (Chung and Fabbri, 1999), neurofuzzy systems of analysis (Elias and Bandis, 2000), or factor scoring of regression parameters (Gorsevski et al., 2000), all of which yield an absolute or relative probability of slope failure. For physically based models it is possible to derive predictions through simulation based on estimated parameter variability (Benda and Dunne, 1997; Terlien et al., 1995). Repeated simulations based on the spatial and statistical variability of input parameters yield a hazard zonation map in which each grid cell is associated with a predicted probability of failure.

The issue of scale in the implementation of an environmental model has received considerable attention in recent years (e.g., Miles et al., 2000; Miles and Ho, 1999; Heuvelink and Pebesma, 1999; Zhang et al., 1999; Fiedler and Ascough, 1998). In landslide modeling, however, little has been written on the problem of scale in model evaluation. Maps of landslide hazard are produced at a wide range of scales and detail, reflecting the needs of the project (Carrara et al., 1991), the availability of detailed data (Montgomery and Dietrich, 1994; Dunne, 1998), and the quality of the historic landslide inventory (Carrara et al., 1992). The scale at which observed instability is mapped also varies, ranging from point locations or single grid cells (e.g., Wang and Unwin, 1992; Pack et al., 1998b) to depiction of the areal extent of slide zones (e.g., Montgomery and Dietrich, 1994; Harp and Jibson, 1995) to broadly delineated slope units or zones of landslide activity (e.g., Carrara et al., 1991).

With few exceptions (e.g., Carrara et al., 1991) no rigorous effort has been made to match the scale of mapped instability to the scale of physical variability captured by the prediction model. Thus models are evaluated on the basis of "percent hit rate" or count density in the absence of any evidence that this metric represents more than fortuitous coincidence or black-box correlation with other variables (Miles et al., 2000). While it is never possible to prove the "validity" of an environmental model (Oreskes, 1998), it is necessary to account for spatial bias or autocorrelation in any measure of model performance.

Slope failure is a complex physical process, and no model fully accounts for causal processes (Carrara et al., 1992). This is especially true in the tropics, where localized weathering and subsurface flow can have a dominant influence on slope stability but are nearly impossible to map at the watershed scale (Simon et al., 1990). When landslides are triggered by local processes not accounted for in the physically based model (e.g., faults in the bedrock), the spatial distribution of observed slope failures will differ from the spatial structure of model predictions. In particular, landslides are often clustered because of interaction or mutual correlation with a single destabilizing process. This clustering can introduce spatial bias into the evaluation process, compromising model assessment. It is possible to capture differences in spatial structure between model predictions and reality, and subsequently to adjust the resolution of the test data set to match the scale of physical

processes modeled, by characterizing the landslide phenomena as a spatial-point process (Cressie, 1991) and analyzing it as such.

The objectives of this research were to implement a physically based landslide model (SINMAP, Pack et al., 1998a) in an agricultural region of Honduras and to demonstrate methods for the representation of uncertainty and spatially unbiased evaluation of a GIS-based landslide model.

MATERIALS AND METHODS

Study Area

The study area comprises three contiguous watersheds in the central highlands of Honduras (Fig. 1), those of the Rio Salitroso, the Rio Frio, and the headwaters of the Rio Quirima. All three rivers drain into Embalse Francisco Morazán—the reservoir of the largest hydroelectric dam in the nation, which provides Honduras with the majority of its electricity (Mangurian, 1997) but is rapidly silting in (COHDEFOR, 1998; IADB, 1999). The study area lies within the municipality of La Libertad, Distrito Comayagua (14° 47' N lat., 87° 35' W long.), and covers an area of 46.1 km². Terrain is steeply dissected, with residual soils on upland areas and associated colluvium in valley bottoms. Soils are weathered from volcanic rock (basalt and andesite flows) in the northern portions of the study area and from sedimentary formations (redbeds and calcareous shales) in the center and south (Fig. 1). Land use in the project area is predominantly agricultural, with coffee cultivation (*Coffea arabica* L.) dominating upland areas and lowlands divided between cattle pasture and the production of maize (*Zea mays* L.) and beans (*Phaseolus vulgaris* L., *Phaseolus lunatus* L.). Most farms are between 1 and 2 ha in size and are cultivated by the landowner (COHDEFOR, 1998).

The central Honduran highlands are semi-humid tropical, receiving an average of 1900 mm of precipitation annually, concentrated in a moderate rainy season from May to July and a heavy rainy season from September to November. Hurricane Mitch inflicted severe damage on the study area, triggering significant debris flows, mudslides, surface erosion, lowland flooding, and the consequent destruction of numerous homes and farms (Cruz and Reyes, 2000).

Data Collection

Elevation contours were hand digitized in ArcView GIS (ESRI Inc., Redlands, CA) from 1:50 000 topographic basemaps (NIMA, Fairfax, VA). These contours were used to interpolate a raster DEM at the 5-m scale (after Zhang and Montgomery, 1994). Information on slope and flow accumulation was, in turn, derived from the DEM. Flow accumulation was calculated from specific catchment area (upslope area per unit contour length [$L^2 L^{-1}$]) according to a model of saturation from below that routes all flow along topographic gradients, assumes steady-state recharge, and uses a value for hydraulic conductivity that is constant with depth (Pack et al., 1998a).

A total of 63 soil samples were collected from the 0.10- and 0.75-m depths for the research area, covering the A and B/C horizons for the range of observed soil and land cover types. Only samples from the B/C horizons were used in the analysis of soil properties for this study. Saturated bulk density (ρ_s), oven-dried bulk density (ρ_d), and saturated shear strength (τ_{sat}) (Torvane Shear Strength Device, ELE International, Lake Bluff, IL) were recorded for each sample. Soil cohesion (c) was calculated from saturated shear strength measurements

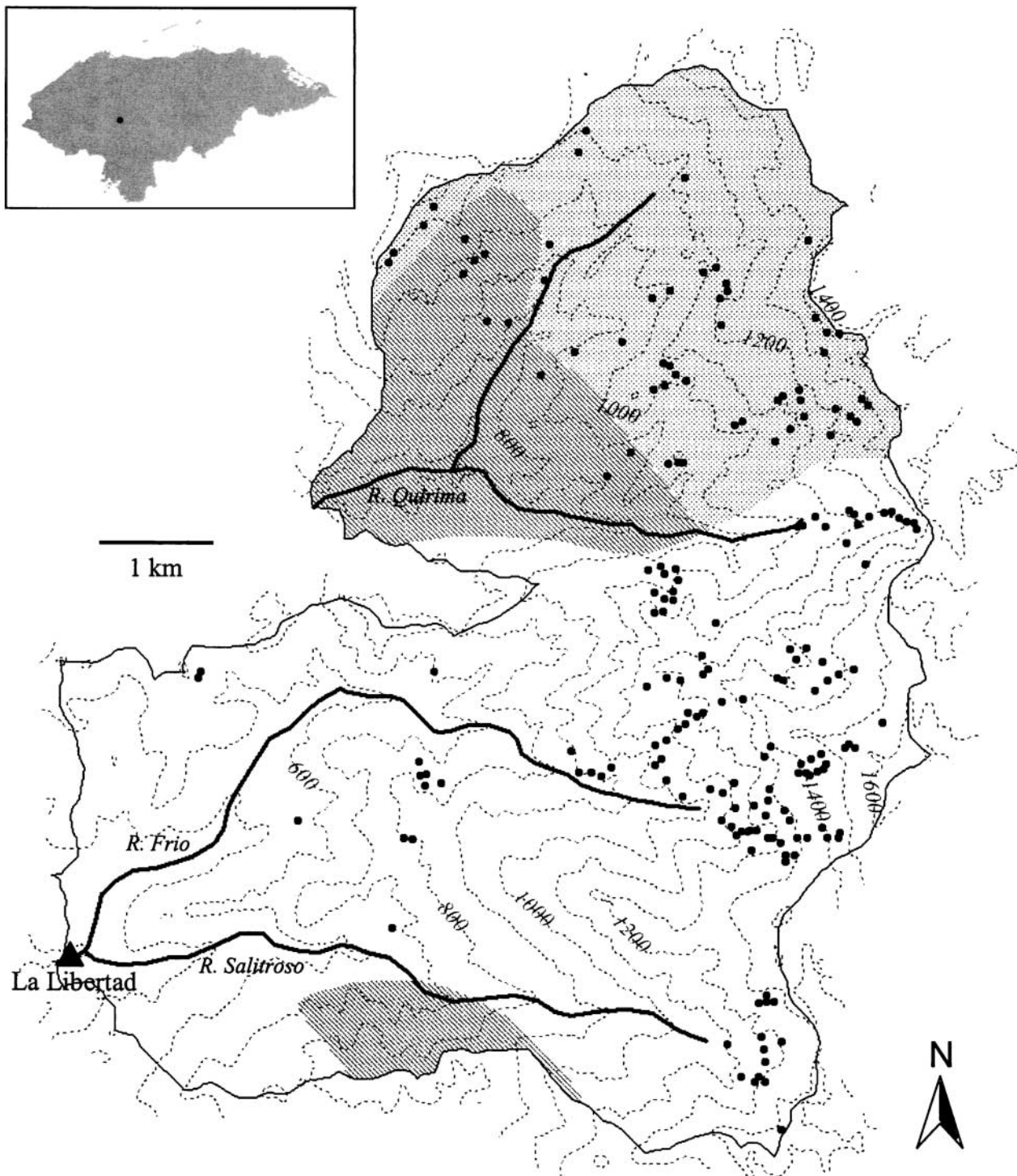


Fig. 1. The study area comprises three contiguous watersheds: Upper Quirima, Rio Frio, and Rio Salitroso. Shading indicates the three geologic units: the Matagalpa Formation (dots), the Yojoa group (white), and the Valle de Angeles group (lines). Points are locations of observed slope failure. The town of La Libertad, in the southwest corner of the study area, is located at $14^{\circ} 45' 24''$ N lat., $87^{\circ} 36' 42''$ W long.

using the European Soil Erosion Model (EUROSEM) correction factor to convert saturated torvane measurements to soil cohesion values (Zimbone et al., 1996; Morgan et al., 1993). This method fails to capture the full influence of roots on cohesion, as the torvane device is too small to register cohesion at the scale of large root effects. In this regard the estimate of c is conservative and shows little correlation with surface vegetation. Angle of soil friction for the samples (ϕ) was corre-

lated with soil texture (feel method; Brady, 1990, p. 95–97), bulk density, and porosity by the U.S. Navy graphical method (U.S. Navy, 1986, p. 148). The method is designed for noncohesive soils, such as clean sands and gravels. There is, therefore, some approximation involved in applying the correlation to soils that contain fines. This approximation was deemed appropriate because all soil cores exhibited very low cohesion when saturated (see Table 1, Results). Such low cohesion

Table 1. Mechanical and hydrologic parameters used in the slope stability model.

Parameter	Rock group	<i>n</i>	mean	Range	SD†
ρ_{sat} , Mg m ⁻³	Yojoa Group	8	1.83	1.80–1.86	0.027
	Valle de Angeles Group	8	1.69	1.63–1.72	0.044
	Matagalpa Formation	14	1.74	1.67–1.85	0.066
ϕ , °	Yojoa Group	8	31.8	35.1–28.6	3.20
	Valle de Angeles Group	8	29.3	30.4–29.1	0.97
	Matagalpa Formation	14	28.7	25.6–31.7	2.94
<i>c</i> , kPa	Yojoa Group	8	0.099	0.060–0.132	0.035
	Valle de Angeles Group	8	0.089	0.040–0.131	0.044
	Matagalpa Formation	14	0.062	0.032–0.100	0.024
log <i>K</i> _{sat} , m s ⁻¹	Yojoa Group	8	-3.97	-4.44–-3.74	0.34
	Valle de Angeles Group	8	-4.52	-4.76–-4.20	0.27
	Matagalpa Formation	14	-4.73	-5.22–-4.17	0.39
<i>D</i> , m	Yojoa Group	8	3	1.50–4.50	-
	Valle de Angeles Group	8	1	0.50–1.50	-
	Matagalpa Formation	14	3.25	1.50–5.00	-
Texture (USDA)	Yojoa Group	37	loam, sandy loam		-
	Valle de Angeles Group	31	loam, sandy clay loam		-
	Matagalpa Formation	53	sandy clay loam		-
		Area km ²	No. landslide systems	Slide density km ⁻²	
	Yojoa Group	29.03	43	1.48	
	Valle de Angeles Group	8.06	8	0.99	
	Matagalpa Formation	9.00	30	3.33	

† Standard deviation.

values are typical for normally consolidated, noncemented clayey sands and sandy clays, and these soil types are conventionally treated as noncohesive for calculations of ϕ (Holtz and Kovacs, 1981). Saturated hydraulic conductivity (K_{sat}) was evaluated with the falling head method (Reynolds, 1993) for 76-mm undisturbed soil cores, based on the average of three trials per sample. The thickness of soil above bedrock (*D*) was measured at 50 points (road cuts and in sample pits) for each lithologic group using judgment sampling.

Three major soil types were identified in the study area and their distribution was mapped through correlation with surface lithology, which was obtained from 1:500 000 USGS geologic maps for Honduras. Field survey information was used to refine the map, as data were deaggregated to match the scale of the DEM. Deaggregation is known to introduce uncertainty to a spatial model (Heuvelink and Pebesma, 1999), but, when the process is justified with field observations, it allows the modeler to present more detailed, intuitive results for use in prediction and management (Miles et al., 2000; Montgomery and Dietrich, 1994). Lithologic types include limestone deposits (Valle de Angeles Group), pyroclastic rock (Matagalpa Formation), and calcareous shale (Yojoa Group). Soils of the Yojoa Group and Matagalpa Formation are weakly developed Ustorthents and Troporthents. The Valle de Angeles Group contains small deposits of Haplustalfs and Argustolls in addition to Ustorthents. Properties measured from soil samples were grouped by lithologic type to provide calibration parameters for the stability model.

No reliable data on rainfall from Hurricane Mitch are available for the study area, and, because of the highly destructive nature of the storm, data from rainfall gauges throughout Honduras are of questionable quality (Hellin and Haigh, 1999). Maximum 30-min intensities of 71 mm h⁻¹ were reported from the South of the country (Hellin and Haigh, 1999) while a sustained intensity of nearly 107 mm h⁻¹ was recorded over one 6-h period in the North (McCown et al., 1998). A steady-state recharge rate of 76 mm h⁻¹ was used for modeling purposes, considered conservative for maximum, multiple hour sustained rainfall intensity in Central Honduras.

An inventory of recent landslides in the study area was established through a field survey in September 2000 and the interpretation of 1:40 000 black and white aerial photographs

(USGS, Washington, DC) taken in March 2000. All landslides were mapped at the head scarp of the slope failure (after Pack et al., 1998a). Point mapping was considered to be the most appropriate inventory method for both practical reasons (dense vegetation in the tropics introduces considerable uncertainty to aerial slide interpretation) and mechanistic concerns—volcanic soils may liquefy when disturbed, leading to large mudslides that are only a secondary consequence of initial slope failure (Terlien et al., 1995). It is likely that the landslide inventory underestimates the number of small slope failures, which can be difficult to identify on aerial photos.

Model Implementation

Following Montgomery and Dietrich (1994) a physically based slope stability model was used in this study. Physically based models are useful in that they allow for relatively fine scale hazard mapping (Pack et al., 1998b) and tend to be less site specific than multivariate statistical analyses (Montgomery and Dietrich, 1994). The infinite slope stability approach is commonly applied in a GIS environment (e.g., Hammond et al., 1992; Montgomery and Dietrich, 1994; Wu and Sidle, 1995; Terlien et al., 1995; Pack et al., 1998a) and evaluates slope stability based on an estimated potential for failure, expressed as (Hammond et al., 1992):

$$FS = \frac{c + \cos^2\theta[\rho_s g(D_p - D_w) + \rho_s g - \rho_w g]D_w}{D_p \rho_s g \sin\theta \cos\theta} \tan\theta$$

Where FS is the factor of safety for slope stability, for which values <1 represent failure conditions. Parameter *c* is soil cohesion (ML⁻¹ Mg⁻²), θ is the local slope gradient, ρ_s is the saturated bulk density of the soil (ML⁻³), ρ_w is the unit density of water, *D_p* is the thickness of soil above the failure plane (L), *D_w* is the thickness of saturated soil above the failure plane, ϕ is the soil angle of friction, and *g* is the acceleration because of gravity (L M⁻²).

The depth of soil above the failure plane *D_p* was assumed to equal the total depth of soil to bedrock, *D*. This condition does not always hold for plastic soils, where diverse failure mechanisms are possible (see e.g., Royster, 1979). Nonetheless, the infinite slope model with the assumption of failure

at the soil–bedrock interface was deemed appropriate because: (i) the algorithm tends to be conservative for situations of deep-seated failure (Terlien et al., 1995) and (ii) according to a poststorm survey mud and debris flows in the study area generally initiated as translational soil slips (Cruz and Reyes, 2000).

Pack et al. (1998a) implemented an adaptation of this equation in the SINMAP model, which is available as a freeware extension for ArcView GIS. Stability index mapping models shallow translational landslides by combining the infinite slope stability equation with a steady-state hydrology model that calculates depth of saturation based on water recharge rate and soil transmissivity. Required parameters at each node are ϕ , K_{sat} , D , steady-state rainfall rate, and dimensionless soil cohesion C^* , defined as:

$$C^* = \frac{c}{D_p \cos\theta \rho_s g}$$

In numerous applications SINMAP has proven to be an effective tool for the rapid identification of potentially unstable zones in large land areas (Pack et al., 1998b).

Parameter Uncertainty

Stability index mapping accounts for parameter uncertainty through the use of uniform probability distributions for certain input parameters (Pack et al., 1998a). This capacity was not used, however, because some parameters do not follow a uniform distribution in the field. The saturation hydraulic conductivity is generally distributed log normally, while values for saturated bulk density, saturated shear strength, and porosity (and thus angle of friction) are approximately normally distributed (Kempthorne and Allmaras, 1986). To capture true uncertainty we calculated the mean value and the value at ± 0.25 standard deviation (SD), ± 0.5 SD, ± 1.0 SD, and ± 2.0 SD for each normally distributed parameter and for the log of K_{sat} (after Snedecor and Cochran, 1980, on small-sample distributions). The distribution of D could not be characterized, so a uniform distribution was assumed, with representative mean. Deterministic SINMAP simulations for all combinations of input parameter values were performed to identify model sensitivity. It was found that the FS calculation was most sensitive to K_{sat} and ϕ , and the joint probability of failure was defined as probability that $FS < 1$ given the estimated field variability of K_{sat} and ϕ . A DPM of the study area was derived from the spatial distribution of these probability predictions. Probabilities reported in the DPM do not take into account uncertainties in the DEM (e.g., erroneous values of slope gradient), in the estimate of rainfall rate (which was held constant), or in the U.S. Navy correlation method used to obtain ϕ (SD for ϕ was derived graphically from measured distributions in ρ_s and porosity and from observed variability in soil texture).

Spatial Randomness and Aggregation

To quantify the scale at which clustering of landslides takes place and relate that to various methods of aggregating the observations, it is useful to generate statistical summarizations of simulated realizations from the DPM and compare those with the observed data similarly aggregated. To do this, the simulated data are derived for the region via Monte Carlo simulation using the probabilities given by the DPM conditioned on the number of landslides observed. The simulation algorithm is as follows. First, a geographic location is randomly selected on the map. This is typically accomplished by selecting the x coordinate of the location from a uniform distribution

on the range of x , followed by a y coordinate selected in the same manner. The result is a random (Poisson) scatter of points over the map. Once the location is selected, a third random variate (z) representing a potential landslide realization is generated from a uniform distribution on (0,1). If the value of this realization is greater than the predicted probability of a landslide occurrence from our DPM (i.e., if $z > p$ [landslide | x, y]) then we keep the location as a realized (simulated) landslide and go on to the next randomly generated location until a total of 190 landslides (equaling the number observed originally) have been generated. The single observed (true) realization is then compared with the distribution of 1000 randomly generated realizations as a test of the null hypothesis that the observed data came from the assumed distribution. The product of this algorithm is a set of points that is uncorrelated with the set of observed slides but that has a nonrandom spatial structure that is similar to that of the DPM. This process makes it possible to compare what the DPM predicts to what has been observed in a spatially unbiased manner.

Because the observations (i.e., the set of landslide locations) are not a single point, as in the typical hypothesis testing framework, but are an array a spatial observations across a broad geographic scale, Ripley's K -function (Ripley, 1976; Venebles and Ripley, 1999) can be used characterize the spatial distribution of points across scales. This statistic characterizes the spatial distribution of points by calculating the expected number of observations within a distance d of a given observation:

$$K(d) = \lambda^{-1} E[\text{number of additional points within distance } d \text{ of an arbitrary point}]$$

Where λ is global intensity, taken here to be the density of landslides per unit area (Cressie, 1991).

To simplify the presentation only the 25th, 501st, and 975th ranked realizations summarized by $K(d)$ are given, representing the 2.5th, 50th, and 97.5th percentiles of the distribution, or roughly the median and 95% confidence bounds of the distribution. Empirical $K(d)$ values for the test data set were plotted alongside these realizations, and deviations of the test data from the simulation envelope were taken to represent spatial structure not accounted for by the model at the interpoint distance (d) of deviation. The empirical $K(d)$ was also calculated for test data grouped into landslide events that included all failure scarps mapped within 100, 150, and 200 m of each other. For each analysis the total number of landslide events was different (larger grouping radii lump slope failures into fewer defined slide systems), and λ was adjusted accordingly.

RESULTS AND DISCUSSION

A total of 190 storm-induced landslides were identified in the study area. Slide density was greatest in the deep residual soils of the Matagalpa Formation, at 3.33 km^{-2} , moderate in the Yojoa Group (1.48 km^{-2}), and lowest in the relatively shallow soils of the Valle de Angeles Group (0.99 km^{-2} ; Table 1). Mapped slope failures were not distributed evenly across the study area. Slide frequency was greatest in upland regions, and individual failure scarps were clustered at river heads and in the areas immediately surrounding large landslide events (Fig. 1).

Parameter Uncertainty

Measurements of soil strength and hydrologic properties showed substantial variability both within and between lithologic groups (Table 1). Soils overlying the calcareous shales of the Yojoa Group were deep and had high hydraulic conductivities ($D = 3$ m, $K_{\text{sat}} = 1.06 \times 10^{-4}$ m s $^{-1}$). These soils were predominantly sand silt mixtures (USDA loam and sandy loam) and had low saturated cohesion (0.099 kPa). Mean ϕ was 31.8°. Soils of the Valle de Angeles group were clayey fine sands (USDA loam and sandy clay loam), were relatively shallow ($\phi = 29.3^\circ$, $D = 1$ m), and had lower average K_{sat} (3.02×10^{-5} m s $^{-1}$). Saturated cohesion was low (0.089 kPa). Soils of the Matagalpa Formation were deep ($D = 3.25$ m), highly weathered, clayey sands (USDA sandy clay loam). These deposits had the lowest K_{sat} (1.86×10^{-5} m s $^{-1}$) and ϕ (28.6°). Measurements of shear strength in the field demonstrated that these soils could exhibit cohesion under nonsaturated conditions (data not shown) but cohesion was found to be very low (0.062 kPa) for saturated soil cores.

Total area predicted to be unstable (FS < 1) was most sensitive to variability in the parameters ϕ and K_{sat} . Manipulation of each parameter to ± 2.0 SD of the field-recorded mean (i.e., 95% of total expected variability) effected a change of up to 19 and 17%, respectively, in the total area predicted to be unstable. In both cases, model sensitivity was greatest for low-end parameter values. Model sensitivity was insignificant to variability in ρ_s (<1%), and manipulation of parameters c and D resulted in only a 3 and 2% maximum change, respectively, from the area predicted to be unstable using mean values. Relative insensitivity to cohesion and soil thickness result from the low values we obtained for saturated soil cohesion, and is not inherent to SINMAP or to the infinite slope stability model (e.g., Gray and Megahan, 1981).

Joint sensitivity to ϕ and K_{sat} amounted to a range of

nearly 53% in the fraction of total area predicted to be unstable (Fig. 2). Most of this variability, however, occurred at the outward edges of parameter distribution; for the middle 68% of the joint distribution of ϕ and K_{sat} total model sensitivity was <7%. The sensitivity to high and low end combinations of these parameters is cause for some concern, however, as both are highly variable in the field (Grayson et al., 1992; Kempthorne and Allmaras, 1986). For this reason a conservative interpretation of model output is recommended. Moreover, uncertainties in the correlation method used to obtain ϕ could not be quantified, and it is likely that real uncertainty in this parameter is even greater than reported on Table 1. Most importantly, the graphical method provides no guidelines for quantifying soil texture, though this is a key variable in developing correlations between porosity and angle of friction. The use of categorical description makes the method conducive to rapid field survey, but this comes at the price of unidentified uncertainty in the estimate. The development of better field methods for estimating angle of friction is desirable. Failing this, more intensive sampling of the parameters used to estimate ϕ is recommended for future studies.

Probabilities associated with model sensitivity to ϕ and K_{sat} are presented spatially in the DPM for the study area (Fig. 3). Probability classes reflect the joint statistical distribution of ϕ and K_{sat} and map shading indicates the spatial distribution of model predictions. Predictions of relative stability across the study area (i.e., which zones had the highest probabilities of failure) were not sensitive to parameter adjustments. This is to be expected, as the relative stability assessment is governed by specific catchment area, through its influence on soil wetness (O'Loughlin, 1986) and local slope gradient (Pack et al., 1998a). Only the absolute magnitude of the stability index is governed by soil properties at the point of analysis.

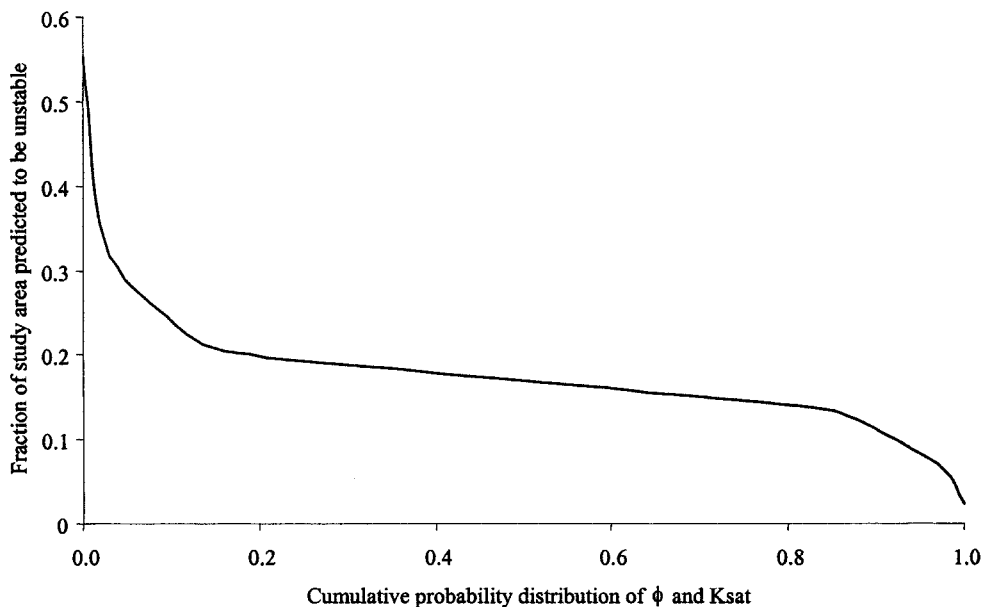


Fig. 2. Fraction of the total study area that is predicted to be unstable over the joint distribution of ϕ and K_{sat} .

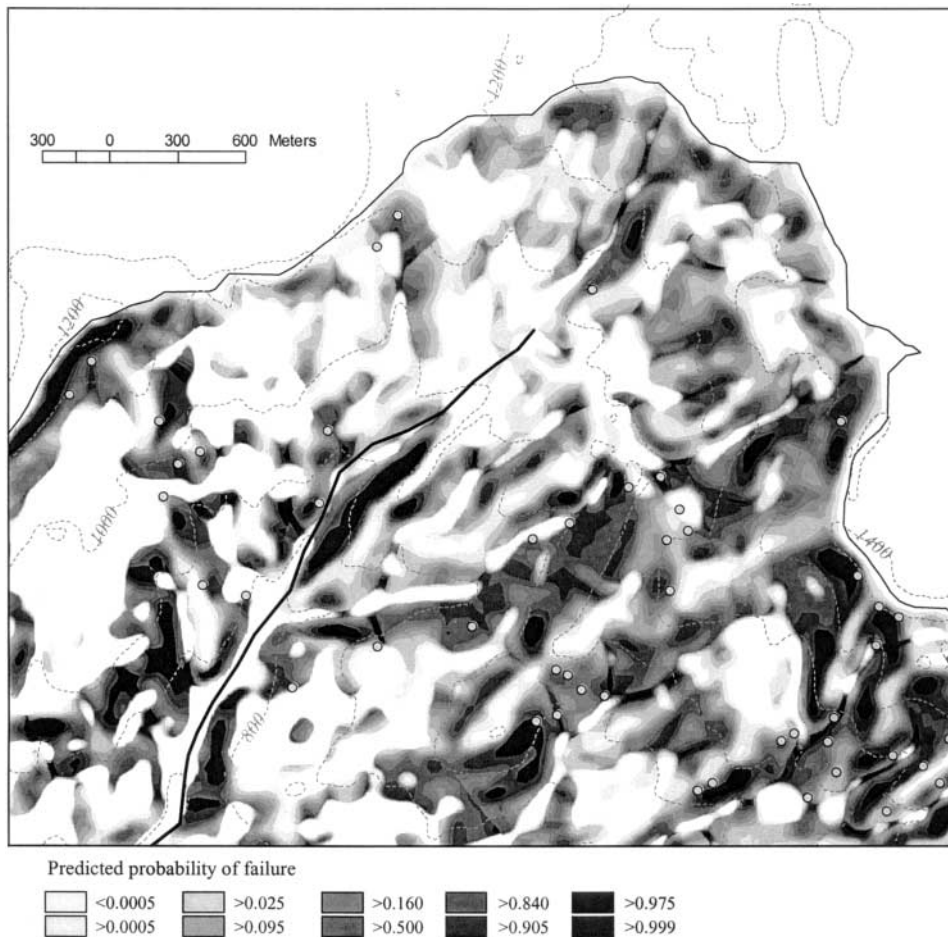


Fig. 3. Cumulative probability map for a portion of the Upper Quirima watershed.

Spatial Randomness and Aggregation

The spatial distribution of mapped landslide points, described through Ripley's K -function, clearly deviates from random at every scale within in the study area. The thick solid line in Fig. 4a represents the expected intensity of a randomly distributed spatial point process of 190 events within the study area. As distance from a given event increases, the total number of events encountered increases according to the Poisson distribution. Thin lines above and below the intensity expectation represent a 95% confidence interval based on 1000 simulations of the random process. The trail of solid dots indicates intensity for actual observations of landslide events in the test data set (190 total). The fact that $K(d)$ is greater for observed slides than it is for random points at distances from 0 to 4000 m indicates that there is significant spatial clustering of landslide events. This is expected, as it is the very nonrandom nature of landslide susceptibility that allows us to evaluate and model the phenomenon.

By considering spatial variability in slope gradient, specific catchment area, and parameters of soil strength and hydrology, SINMAP captures a significant fraction of observed clustering (Fig. 4b). Solid points still indicate the distribution of observed landslide systems, but lines represent the mean and 95% confidence interval

for 1000 simulations of 190 spatially independent points selected according to predicted probability of failure (see Materials and Methods). The $K(d)$ values for observed slides now fall within the simulation envelope at all distances >1500 m. For small distances, however, clustering is greater for the test data set than it is for the 95% simulation envelope of independent SINMAP predictions (Fig. 5a). This indicates that the model does not account for all processes responsible for local clustering and that it is necessary to aggregate observations in the mapped landslide inventory for purposes of model evaluation.

The most likely sources of clustering at <1500 m are landslide interaction (i.e., one slope failure directly triggers another) and mutual correlation with a locally destabilizing landscape feature such as uneven weathering, road construction, or an undercut river. In cases of interaction or mutual correlation it is appropriate to group slope failures together into landslide systems that stem from a single combination of destabilizing factors. Given high quality aerial photography or timely post-storm survey, it is possible to perform expert identification of landslide correlation (e.g., Carrara et al., 1992; Wang and Unwin, 1992). Considering the well-documented subjectivity of such analyses, however (Carrara et al., 1992), and the limited availability of cloud-free

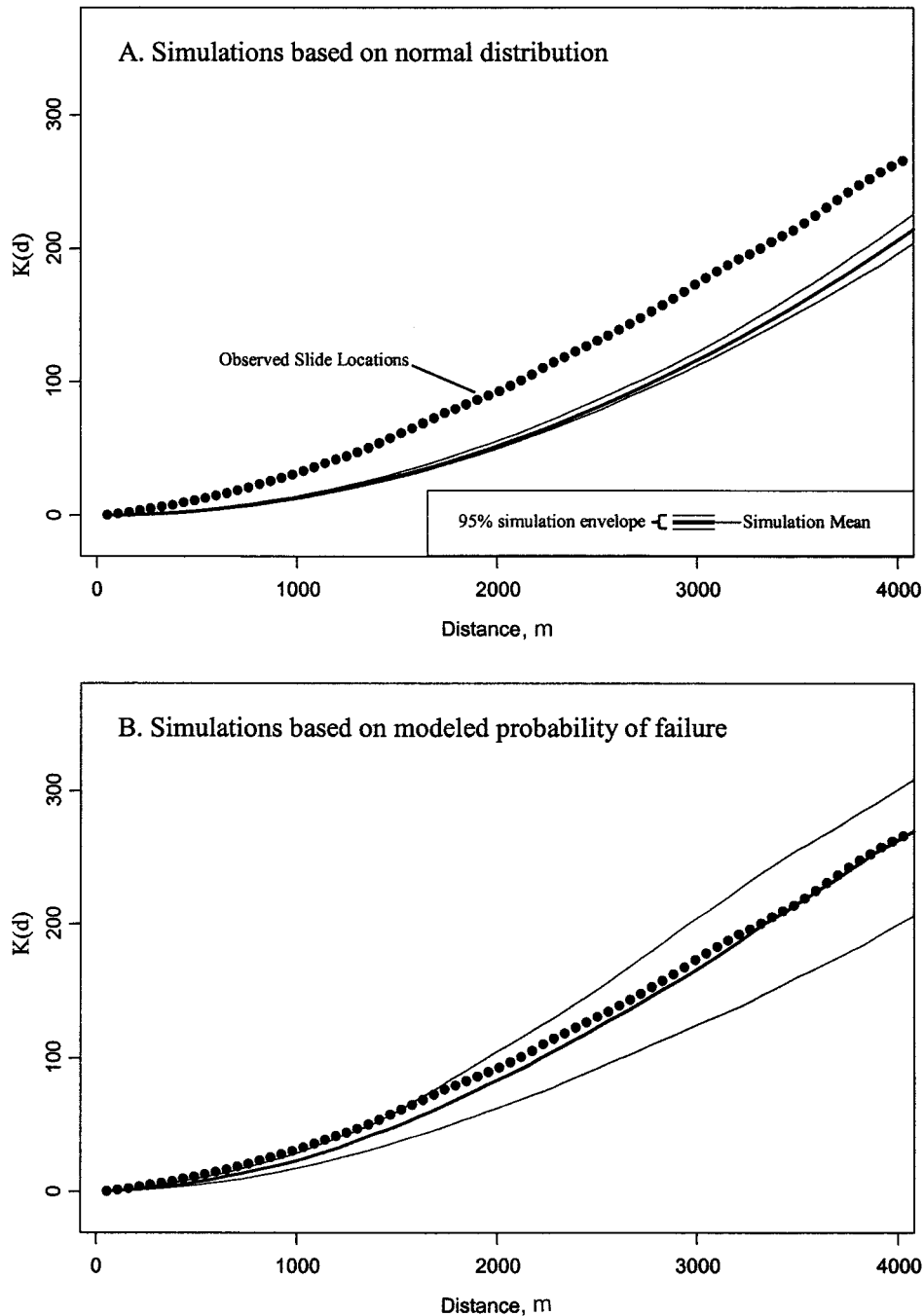


Fig. 4. Ripley's K -function for mapped landslide inventory (dotted line) and for the mean and 95% simulation envelope (solid lines) for 1000 simulations of (A) 190 normally distributed points and (B) 190 points selected according to modeled probability of failure.

imagery in the wake of Hurricane Mitch, an automated criterion was used: all mapped failures that lie within a given distance of each other were deemed to be potentially correlated, and multiple grouping was allowed (i.e., a mapped failure could be potentially correlated with more than one neighboring failure). Through repeated simulations of the K -function we found that an aggregation distance of 150 m was required to account for fine-scale spatial structure in the test data set (Fig. 5 b,c). Aggregation distances <150 m overgeneralized the landslide inventory, washing out local structure in slope and saturation that the model does take into account

(Fig. 5d). Aggregation did not affect $K(d)$ for distances >1500 m.

Using the 150 m proximity rule, the 190 mapped failure scarps were grouped into 81 landslide systems. Each failure scarp was then associated with a 35-m buffer to account for mapping uncertainty in the empirical evaluation process (after Carrara et al., 1992). We found that 61 landslide systems—75% of the population—overlapped a zone of moderate failure potential (probability ≥ 0.5 for Hurricane Mitch conditions). Of these, 42 slide systems—52% of the population—overlapped a zone of very high failure potential (probability ≥ 0.975

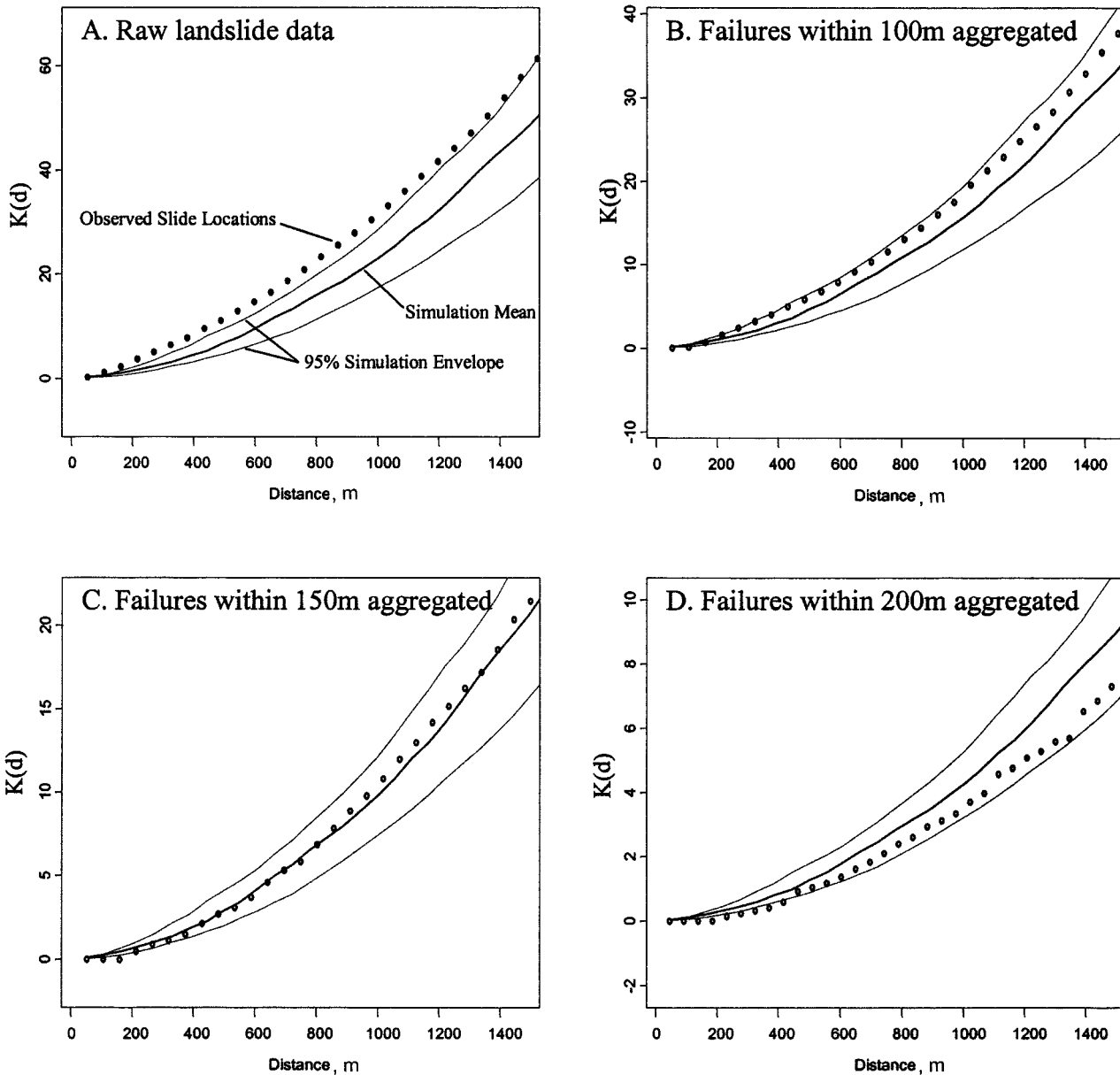


Fig. 5. Ripley's K-function for mapped landslide inventory (dotted line) and for the mean and 95% simulation envelope (solid lines) for 1000 simulations of 190 points selected according to modeled probability of failure. In (A) the landslide inventory is unedited. In (B) all failure scarps within 100 m of each other have been aggregated into landslide systems. In (C) failure scarps within 150 m have been aggregated, and in (D) failure scarps within 200 m have been aggregated.

for Hurricane Mitch). In total 16.9% of the study area was classified as moderate, and 6.4% as very high failure potential during Mitch (Table 2).

CONCLUSIONS

Our objective was to apply a spatially distributed slope stability model to an area affected by Hurricane Mitch. SINMAP, a model that utilizes a steady state hydrology model, the infinite slope stability model and GIS data structures, performed well in the study area, assigning a probability of failure of <0.975 to 52% of identified landslide systems and a probability of failure <0.5 to 75% of identified systems. A 75% identification rate is roughly comparable with the successes reported

in other landslide modeling efforts (e.g., Carrara et al., 1992; Montgomery and Dietrich, 1994; Chung et al., 1995; Pack et al., 1998a; Iida, 1999; Gorsevski et al., 2000). There are certainly examples of higher accuracy model applications (e.g., Montgomery and Dietrich, 1994; Pack et al., 1998b), but this study can be considered a success for GIS-based modeling in a region with little biophysical information available.

Two issues significant to environmental modeling in general were encountered in the course of this study. First, given the variability associated with most environmental parameters, it is important to incorporate uncertainty into any report of model output (Pack et al., 1998a; Terlien et al., 1995). Presenting model predictions as a DPM is an information-rich and statistically

Table 2. Evaluation statistics for the distributed probability map.

Predicted probability for slope failure	Area	% of total area	No. slide systems	% of total slide systems	Slide system density
<0.005	20.61	44.74	5	6.17	0.24
0.005–0.025	10.05	21.80	6	7.41	0.60
0.025–0.095	4.11	8.91	5	6.17	1.22
0.095–0.160	1.86	4.04	1	1.23	0.54
0.160–0.500	1.69	3.66	3	3.70	1.78
0.500–0.840	1.47	3.18	7	8.64	4.77
0.840–0.905	1.32	2.87	2	2.47	1.51
0.905–0.975	2.03	4.39	10	12.35	4.94
0.975–0.999	1.89	4.10	21	25.93	11.13
>0.999	1.06	2.31	21	25.93	19.73

rigorous method for doing this. The concept of probability of failure under specified storm conditions is meaningful and intuitive to the end-user.

Second, the issue of scale cannot be ignored in the empirical evaluation stage of a modeling project. Spatial structure in a test data set that occurs on a scale smaller than the variability captured by the model indicates that (i) there are physical processes unaccounted for by the model, such as interaction between landslides, or (ii) variability of parameters that the model does take into account (e.g., soil depth) occurs at a scale finer than that captured by input data. When either of these apply, the test data set must be aggregated to a coarser resolution to allow for spatially unbiased evaluation of the model. In this application small-scale structure did exist in the test data set. Using Ripley’s *K*-function allowed for the adjustment of the landslide inventory to a resolution appropriate for model evaluation.

In keeping with Oreskes (1998), the term *validation* was avoided in reference to model performance. Instead an innovative approach to empirical model *evaluation* was used that accounts for parameter variability and model scale specific to each application. Empirical evaluation is not, however, the end goal of a hazard model. The true value of a model can only be assessed in conversation with decision-makers and stakeholders in the study area (Miles et al., 2000).

ACKNOWLEDGMENTS

The authors thank the Cornell Institute for International Food and Agriculture Development (CIIFAD) for sponsoring this research, and Teratech Consulting Ltd. (Salmon Arm, BC, Canada) for making the SINMAP model available.

REFERENCES

Alexander, D.E. 1995. A survey of the field of natural hazards and disaster studies p. 1–19. *In* A. Carrara and F. Guzzetti (ed.) Geographical information systems in assessing natural hazards. Kluwer Acad. Pub., The Netherlands.

Benda, L., and T. Dunne. 1997. Stochastic forcing of sediment supply to channel networks from landsliding and debris flow. *Water Resour. Res.* 33:2849–2863.

Bergin, D.O., M.O. Kimberley, and M. Marden. 1995. Protective value of regenerating tea tree stands on erosion-prone hill country, East Coast, North Island, New Zealand. *N.Z. J. For. Sci.* 25(1):3–19.

Brady, N.C. 1990. *The nature and properties of soils*. 10th ed. Macmillan, New York.

Carrara, A, M. Cardinali, and F. Guzzetti. 1992. Uncertainty in assessing landslide hazard and risk. *ITC J.* 1992(2):172–183.

Carrara, A., M. Cardinali, R. Detti, F. Guzzetti, V. Pasqui, and P.

Reichenback. 1991. GIS techniques and statistical models in evaluating landslide hazard. *Earth Surf. Process Landforms* 16:427–445.

Chung, C.F., and A.G. Fabbri. 1999. Probabilistic prediction models for landslide hazard mapping. *Photogramm. Eng. Remote Sens.* 65:1389–1399.

Chung, C.F., A.G. Fabbri, and C.J. van Westen. 1995. Multivariate regression analysis for landslide hazard zonation. p. 107–133. *In* A. Carrara and F. Guzzetti (ed.) Geographical information systems in assessing natural hazards. Kluwer Academic Publishers. The Netherlands.

COHDEFOR. 1998. Programa de manejo de los recursos naturales renovables de la cuenca del embalse “El Cajon”: diagnostico general U.O.C. La Libertad. (In Spanish.) Secretary of Natural Resources of Honduras, Tegucigalpa, Honduras.

Coppock, T.J. 1995. GIS and natural hazards: An overview from a GIS perspective. p. 21–34. *In* A. Carrara and F. Guzzetti (ed.) Geographical information systems in assessing natural hazards. Kluwer Academic Publishers, The Netherlands.

Cressie, N. 1991. *Statistics for spatial data*. John Wiley & Sons, Inc., New York.

Cruz, R., and I. Reyes. 2000. Reporte: Efectos del Huracán Mitch a la Cuenca Humuya area de La Libertad (Honduras). (In Spanish.) USDA Foreign Agricultural Service, Washington, DC.

Dunne, T. 1998. Critical data requirements for prediction of erosion and sedimentation in mountain drainage basins. *J. Am. Water Resour. Assoc.* 34(4):795–808.

Elias, P.B., and S.C. Bandis. 2000. Neurofuzzy systems in landslide hazard assessment. p. 199–202. *In* 4th International symposium on spatial accuracy assess in natural resources and environmental science. Proceedings Accuracy, Amsterdam, The Netherlands.

Fiedler, F.R., and J.C. Ascough. 1998. Spatially variable hydrodynamic simulation of overland flow. p. 122–131. ASAE Annual International Meeting, Orlando, FL. 11–16 July 1998. ASAE, St. Joseph, MI.

Gorsevski, P.V., P. Gessler, and R.B. Foltz. 2000. Spatial prediction of landslide hazard using logistic regression and GIS. Paper no. 305. [CD-ROM] 4th International Conference on Integrating GIS and Environmental Modeling, Banff, AB, Canada. 2–8 Sept. 2000. Cooperative Institute for Research in the Environmental Sciences, Boulder, CO.

Gray, D.H., and W.F. Megahan. 1981. Forest vegetation removal and slope stability in the Idaho batholith. *Res. Pap. INT-271*. USDA For. Serv., Portland, OR.

Grayson, R.B., I.D. Moore, and T.A. McMahon. 1992. Physically based hydrologic modeling 2: Is the concept realistic? *Water Resour. Res.* 28:2659–2666.

Guariguata, M.R. 1990. Landslide disturbance and forest regeneration in the Upper Luquillo Mountains. *J. Ecol.* 78:814–832.

Hammond, C., D. Hall, S. Miller, and P. Swetik. 1992. Level I stability analysis (LISA) documentation for version 2.0. Gen Tech. Rep. INT-285. Intermountain Res. Stn., USDA For. Serv., Ogden, UT.

Hansen, A. 1984. Landslide hazard. p. 523–602. *In* D. Brundsen and D.B. Prior (ed.) *Slope instability*. John Wiley & Sons, New York.

Harp, E.L., and R.W. Jibson. 1995. Inventory of landslides triggered by the 1994 Northridge, California earthquake: U.S. Geological Survey Open-File Report 95–213. U.S. Geologic Survey, Reston, VA.

- Hellin, J., and M.J. Haigh. 1999. Rainfall in Honduras during Hurricane Mitch. *Weather* 54(11):350–358.
- Heuvelink, G.B.M., and P.A. Burrough. 1992. Error propagation in cartographic modelling using Boolean logic and continuous classification. *Int. J. Geographical Information Systems* 7:231–246.
- Heuvelink, G.B.M., and E.J. Pebesma. 1999. Spatial aggregation and soil process modelling. *Geoderma* 89:47–65.
- Holtz, R.D., and W.D. Kovacs. 1981. *An Introduction to Geotechnical Engineering*. Prentice-Hall, Englewood Cliffs, NJ.
- Iida, T. 1999. A stochastic hydro-geomorphological model for shallow landsliding due to rainstorm. *Catena* 34:293–313.
- IADB. 1999. Reducing vulnerability to natural hazards: Lessons learned from Hurricane Mitch [online]. Presented to Consultative Group for the Reconstruction and Transformation of Central America. Stockholm, Sweden 25–28 May 1999. Available at http://www.iadb.org/regions/re2/consultative_group/groups/ecology_workshop_1.htm. (verified 9 Sept. 2002.)
- Jibson, R.W. 1993. Predicting earthquake-induced landslide displacements using Newmark's sliding block analysis. *Transp. Res. Rec.* 1411:9–17.
- Kempthorne, O., and R.R. Allmaras. 1986. Errors and variability of observations. *Agronomy* 9:1–31.
- Lal, R. 1994. Global overview of soil erosion. p. 39–51 *In* Baker et al. (ed.) *Soil and water science: Key to understanding our global environment*. SSSA Spec. Publ. 41. SSSA, Madison, WI.
- Lloyd, D.M., M.G. Anderson, and M.A. Othman. 1994. Using a combined slope hydrology/slope stability model for cut slope design in the tropics. *Malaysian J. Trop. Geog.* 25(1):1–10.
- Mahmood, K. 1987. Reservoir sedimentation: Impact, extent, mitigation. Tech. Paper No. 71. World Bank, Washington, DC.
- Mangurian, D. (1997) Ingenuity saves dam [online]. IDB America. Available at <http://www.iadb.org/idbamerica/archive/stories/1997/eng/8d2.htm>. (verified 9 Sept. 2002.)
- McCown, S., A. Graumann, and T. Ross. 1998. Mitch: The deadliest Atlantic hurricane [online]. Available at <http://lwf.ncdc.noaa.gov/oa/reports/mitch/mitch.html>. (verified 9 Sept. 2002.)
- Miles, S.B., and C.L. Ho. 1999. Applications and issues of GIS in civil engineering modeling. *J. Computing Civil Eng.* 13:144–152.
- Miles, S.B., D.K. Keefer, and T.L. Nyerges. 2000. A case study in GIS-based environmental model validation using earthquake-induced landslide hazard. p. 481–492. *In* 4th International symposium on spatial accuracy assessment in natural resource environmental science. Proceedings Accuracy, Amsterdam, The Netherlands.
- Montgomery, D.R., and W.E. Dietrich. 1994. A physically based model for the topographic control on shallow landsliding. *Water Resour. Res.* 30:1153–1171.
- Morgan, R.P.C., J.N. Quinton, and R.J. Rickson. 1993. EUROSEM: A user guide. Silsoe College, Silsoe-Bedford, UK.
- Nagle, G.N., T.J. Fahey, and J.P. Lassoie. 1999. Management of sedimentation in tropical watersheds. *Environ. Manage.* 23:441–452.
- O'Loughlin, E.M. 1986. Prediction of surface saturation zones in natural catchments by topographic analysis. *Water Resour. Res.* 22:794–804.
- Oreskes, N. 1998. Evaluation (not validation) of quantitative models. *Env. Health Perspect.* (suppl.) 106(6):1453–1459.
- Pack, R.T., D.G. Tarboton, and C.N. Goodwin. 1998a. The SINMAP approach to terrain stability mapping. p. 1157–1165. *In* D.P. Moore and O. Hungr (ed.) *Proceedings—International Congress of the International Association of Engineering Geology and the Environment* 8, Vol. 2. 21–25 Sept. 1998. A. A. Balkema, Rotterdam, Netherlands.
- Pack, R.T., D.G. Tarboton, and C.N. Goodwin. 1998b. *Terrain Stability Mapping with SINMAP, technical description and users guide for version 1.00*. Rep. No. 4114-0, Terratech Consulting Ltd., Salmon Arm, BC, Canada.
- Pellek, R. 1989. Contour hedgerows and other soil conservation interventions for hilly terrain. *Agroforestry Systems* 17:135–152.
- Pla, I. 1997. A soil water balance model for monitoring soil erosion processes and effects on steep lands in the tropics. *Soil Technol.* 11:17–30.
- Reynolds, W.D. 1993. Saturated hydraulic conductivity: Laboratory measurement. p. 589–598. *In* M.R. Carter (ed.) *Soil sampling and methods of analysis*. Can. Soc. of Soil Science.
- Ripley, B.D. 1976. The second-order analysis of stationary point processes. *J. Appl. Probability* 13:255–266.
- Roy, A. 2001. Hazard mapping in India: Using GIS for prognostic Himalayan landslide modelling. *GIM International* 15:29–33.
- Royster, D.L. 1979. Landslide remedial measures. *Bull. Assoc. Eng. Geol.* 16:301–352.
- Schuster, R.L. 1994. Socioeconomic significance of landslides. p. 1–11. *In* A.K. Turner and R.L. Schuster (ed.) *Landslides, investigation and mitigation*, Transport Research Board Manual.
- Simon, A., M.C. Larson, and C.R. Hupp. 1990. The role of soil processes in determining mechanisms of slope failure and hillslope development in a humid-tropical forest, eastern Puerto Rico. *Geomorphology* 3:263–286.
- Snedecor, G.W., and W.G. Cochran. 1980. *Statistical methods*, 7th ed. Iowa State Univ. Press, Ames, IA.
- Terlien, M.T.J., C.J. van Westen, and T.W.J. van Asch. 1995. Deterministic modeling in GIS-based landslide hazard assessment. p. 57–77. *In* A. Carrara and F. Guzzetti (ed.) *Geographical information systems in assessing natural hazards*. Kluwer Academic Publishers, The Netherlands.
- U.S. Navy. 1986. *Soil mechanics*. NAVFAC Design Manual DM-7. Washington, DC.
- Venables, W.N., and B.D. Ripley. 1999. *Modern applied statistics with S-PLUS*. 3rd ed. Springer-Verlag, New York.
- Walker, L.R., D.J. Zarin, N. Fetcher, R.W. Myster, and A.H. Johnson. 1996. Ecosystem development and plant succession on landslides in the Caribbean. *Biotropica* 28:566–576.
- Wang, S.Q., and D.J. Unwin. 1992. Modelling landslide distribution in loess soils in China: An investigation. *Int. J. Geographical Information Systems* 6(5):391–405.
- Wu, W., and R.C. Sidle. 1995. A distributed slope stability model for steep forested basins. *Water Resour. Res.* 31:2097–2110.
- Zhang, W., and D.R. Montgomery. 1994. Digital elevation model grid size, landscape representation, and hydrologic simulations. *Water Resour. Res.* 30:1019–1028.
- Zimbone, S.M., A. Vickers, R.P.C. Morgan, and P. Vella. 1996. Field investigations of different techniques for measuring surface soil shear strength. *Soil Technol.* 9:101–111.